

graph is rotated at meridian passage in order to reduce the total flexure, and if the observations are centred on meridian passage the principal result of this shift is to smear the violet end of the spectrum, rather than to create a systematic wavelength dependent velocity shift.

The wavelength calibration is obtained from observations of a Th-Ar lamp. In the reduction process 50 to 70 spectral lines were used to determine the calibration of each echelle order. (Over 10^3 lines are used for wavelength calibrations in the blue green spectral regions). The use of many lines strongly constrains the two dimensional wavelength fit and, to some extent, reduced the calibration errors caused by line blends and misidentifications in the Th-Ar wavelength table. The wavelength calibration process is an iterative one: the first step is to obtain an initial calibration using only the strongest lines. This initial calibration is then used to constrain a second calibration that uses much weaker spectral lines. If the weak lines are used initially, the programme usually finds an incorrect solution for the line fit. But if the wavelength calibration is done correctly, the mean residuals to the fits are about $9 \text{ m}\text{\AA}$ in the blue and $12 \text{ m}\text{\AA}$ in the yellow. In each case this is about $\frac{1}{2}$ pixel or about 0.7 km sec^{-1} .

The motion of the earth can also result in a differential velocity shift of several

km s^{-1} between the beginning and the end of a long integration. The principal effect on the spectrum of the observatories changing velocity vector in space is a reduction of the spectral resolution. A careful choice of the time of observation can mitigate this problem.

If it is intended to convert the observed wavelengths to vacuum values, the formula given by Allen (1964) for the refractive index of air can be used. His formula is valid for standard temperature and pressure and is not strictly correct for the high altitude conditions at La Silla. The difference can amount to about 20 km s^{-1} . The differential effect is approximately 400 m s^{-1} between 4000 \AA and 6000 \AA .

An important feature of the MIDAS extraction programme is that it rebins the raw image pixels to a uniform wavelength scale before merging individual spectral orders. In order not to degrade the spectral resolution of the extracted spectrum, software bin widths of 0.05 \AA can be chosen for the blue spectrum, and for the red 0.10 \AA bin widths were used. Both of these choices result in bins that are narrower than the wavelength span of a single CCD pixel. Unfortunately, the rebinning substantially increases the apparent noise in the spectrum. A discussion of "pattern noise", but in a slightly different context, is given in a paper by Dick et al. (1989). The reduction procedure could be im-

proved if the original CCD pixel width was retained. This would result in a non-uniform wavelength spacing of the pixels. At present, with the available software, this is not possible. Rebinning to a coarser grid than the CCD pixel smooths the data but at the expense of lowering the resolution of the spectrum. I think that some of the even pixel, odd pixel jitter in the spectrum seen in Figure 2 is due to this rebinning pattern noise.

I hope that some of these comments prove useful to the CASPEC user community. A total system efficiency of about 4% can be obtained when using CASPEC! This is rather good for the present state of instrument development. New detectors are on the way, and new instruments and telescopes will make our existing facilities seem modest. But for now CASPEC, if used intelligently, is a powerful tool for widening our understanding of the Universe.

References

- Allen, C.W. 1964, *Astrophysical Quantities* (London: The Athlone Press), p. 144.
 Dick, J., Jenkins, C. and Ziabicki, J. 1989, *Pub. Astron. Soc. Pac.*, **101**, 684.
 D'Odorico, S., Enard, D., Lizon, J.L., Ljung, B., Nees, W., Ponz, D., Raffi, G. and Tanné, J.F. 1983, *The Messenger*, **33**, 2.
 Leach, R.W. 1988, *Pub. Astron. Soc. Pac.*, **100**, 853-858.

More Light Through the Fibre: an Upgrading of the Link 3.6-m – CES

S. D'ODORICO, G. AVILA and P. MOLARO, ESO

1. The Configuration of the Fibre Link Today

Different types of commercial fibre optics find useful application in modern astronomical instruments. ESO has been particularly interested in the use of fibres as "light pipes" to feed spectrographs at a distance from the telescope. This is the case of the Coudé Echelle Spectrograph (CES) fed through a 35 m long fibre from the Cassegrain focus of the 3.6-m telescope, alternatively to the standard use with the CAT telescope. The gain one can achieve by using the larger telescope can be as large as two magnitudes over a wide spectral range and this difference opens the way to an entirely new class of observations that at the CAT would be photon limited. Obviously, would-be observers have to be aware that when the link operates,

both the CAT and the 3.6-m need to be "booked". As a consequence, the OPC checks with special care whether the use of the larger collecting area is indeed absolutely necessary. A very convincing case and an outstanding scientific justification are a must for these programmes.

ESO observers have access to this new observing mode as of April 1988. A complete description of the set-up had been given in the article by Avila and D'Odorico in the Proceedings of the ESO Conference on "Very Large Telescopes and their Instrumentation", p. 1121 (1988). In March 1989 the system was upgraded and we report here on the options which are now available and on the overall efficiency. This information complements what can be found in the March 1989 version of the Operating Manual of the CES.

There are now four fibres permanently installed between the Cassegrain cage of the 3.6-m telescope and the entrance to the CES. Table 1 summarizes the characteristics of the four fibres. Two types of lenses are used on different fibres to image the pupil of the telescope on the fibre input face and change the input ratio from F/8 to around F/3. The rod lenses have a better transmission below 4000 \AA , the self-foc lenses are slightly more efficient between 5000 and 10000 \AA . The transmission of the Polymicro and GFO fibres are approximately equivalent (see Fig. 1); both are used with a 3.4 arcsec diaphragm at their entrance. The smaller core diameter QSF fibre is used with a 2.4 arcsec diaphragm: it has no transmission below 4000 \AA , but it is more efficient than the other two types above 7000 \AA . Three new image slicers are

also available. They are built from silica with transmission around 90% over the entire spectral range. The output end of the working fibre is coupled by a field lens and a triplet to the input face of one of the image slicers. In March 1989 the triplet was also substituted with one made of UV transparent glass with high efficiency over the entire spectral range. The optical system converts the F/3 beam from the fibre to the F/32 beam accepted by the CES collimator. The image slicers "reformat" the image of the fibre into an artificial, narrow long slit. The properties of the different slicers and their optimal coupling to the different fibres and cameras of the CES are also given in Table 1. The resolution on the spectra is determined by the projected width of the slices on the detector. In the March run, using the image slicer #2, we measured an average resolution of 55,000 with the short camera and of 75,000 with the long one.

At the beginning of an observing run with the fibre link, the OPTOPUS adapter is mounted at the Cassegrain focus of the 3.6-m. The fibre of choice is mounted on a special OPTOPUS plate in the central hole of a small mirror, which is used to reflect the light not entering the fibre to the guiding TV. This is normally sufficient to operate the autoguider. On the other end, at the level of the coudé room floor, the fibre, the projection optics and the image slicer replace the mechanical slit at the entrance of the CES. The adjustment of the fibre at the centre of the guiding mirror and at the other end the coupling of the fibre to the image slicer are relatively simple operations which however require time and skill. For this reason they cannot be done during the night.

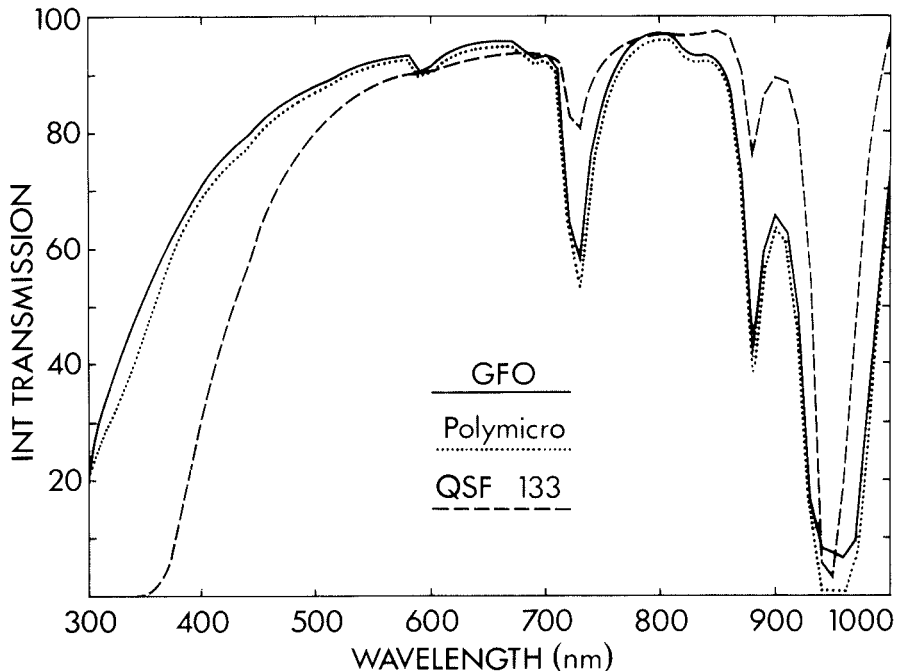


Figure 1: Measured internal transmission of three 35-m fibres used in the link.

Observers are actually asked to identify a single configuration of the link they want to use with a given CES camera to minimize the intervention of the La Silla staff.

2. The Efficiency of the CES Fed by the CAT or by the 3.6-m

The paper by Avila and D'Odorico quoted above included an estimate of the overall efficiency of the link and a measurement in the visible. The internal transmission of the 35-m fibres identified in Table 1 is shown in Figure 1. Additional losses are introduced by the absorption in the various optical com-

ponents of the link and in their interfaces. In order to obtain a set of reliable values, four standard stars were measured in March 1989 both through the link and with the CAT at 6 different wavelengths: 3636, 4030, 5020, 5520, 6460 and 8080 Å. These values were chosen close to the centres of different echelle orders of the CES. The efficiencies at wavelengths far from the blaze can be substantially lower (see Table 2.1 of the CES Operating Manual). The observations in the UV-blue were obtained with the short camera, those in the visible-red region with the long one. For the fibres from the 3.6-m the 3.4-arcsec entrance aperture was used; for the observations with the CAT the entrance slit of the spectrograph was widened to 5 arcsec. The observations were distributed over different nights, all of excellent photometric quality. With both cameras the detector was the standard CES CCD, a double density RCA (ESO #9). The results of this comparative test are shown in Figure 2. The limiting magnitude plotted on the y-axis is defined as the magnitude of a star which at that wavelength produces one photoelectron/Å/sec on the detector. The values were measured for an average seeing of 1.5–2 arcsec and the scatter in the measurements of the different stars was better than +/- .3 magnitudes. From these numbers the observers can easily estimate the exposure times needed to reach a given signal-to-noise ratio. The gain of the 3.6-m over the CAT is consistently around 1.8 magnitude at all wavelengths longer than 5000 Å, it is 1.5 mag at 4000 Å and drops to .65 mag in the UV where the

TABLE 1: Options Available at the Fibre Link

Fibres				
Type	Core diameter	Input ¹	Coupling lens	Recommended use
GFO	200 μ	3.4	rod lens/UBK7	Blue wavel.
GFO	200 μ	3.4	self-foc lens	Red wavel.
Polymicro	200 μ	3.4	rod lens/UBK7	Blue wavel.
QSF	133 μ	2.3	self-foc lens	Red wavel.
Image Slicers				
ESO #	Number of slices	Width ²	Recommended use	
# 1	4	360	Short Camera + QSF fibre	
# 2	7	300	Short and long Camera + GFO or Pol fibres	
# 4	10	270	Long Camera + GFO or Pol fibres	

¹ Diameter of the entrance aperture on the sky in arcsec.

² Approximate width of slices at the entrance of CES in micron.

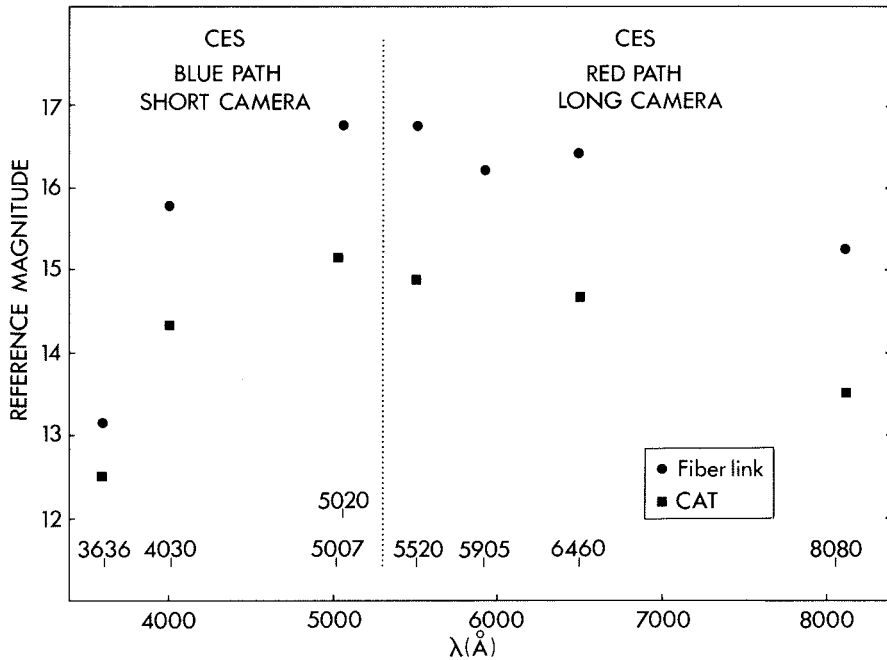


Figure 2: The efficiency of the CES at different wavelengths when fed by the CAT and when used with the fibre link from the 3.6-m telescope. The reference magnitudes on the Y-axis are for stars which give one detected photoelectron/Å/sec.

absorption in the fibre itself is important. The CAT observations were obtained with a 5 arcsec wide slit. The actual gain in a science exposure can be larger than that shown in Figure 2. In medium-poor seeing the narrow slit of the CES will admit less light than the fibre. As an example, with a stellar image of 2 arcsec

FWHM, a typical slit of the CES (1.5 arcsec width, 10 arcsec length) transmits 55% of the light while in the same condition the 3.4 arcsec circular diaphragm transmits 70% of the stellar light.

The measurements have also been used to derive the absolute efficiencies, that is the ratio between the detected

photons and the number of photons falling on the unit surface of the telescope. These numbers take into account the effect of all of the telescope and instrument optics and of the detector. For the measurements with the CAT, these average efficiencies are 0.5, 3.4, 8.6, 9, 7.7 and 2.9 at 3636, 4030, 5020, 5520, 6460 and 8080 Å respectively. The agreement with the values given in the CES Operating manual at slightly different wavelengths is reasonable. The corresponding values from the observations with the 3.6-m and the link are 0.26, 2.1, 6.4, 7, 6 and 2.3 respectively. At wavelengths longer than 4000 Å, the CAT+CES combination is on average 1.3 times more efficient. This advantage is however fully lost when the seeing is 2 arcsec or worse. In those nights the link works at its best and the gain of the larger collecting area is fully realized.

Finally, it is important to call attention to the problems related to the long slit format of the spectra that one obtains with the link. At the beginning of an observing run, the artificial slit produced by the image slicer must be well aligned with the rows of the CCD to avoid a loss of resolution. The use of CCD binning in the direction normal to the dispersion is recommended for those observations where the read-out noise of the CCD (around 30 e/pixel) is a limiting factor. However, binning cannot be too strong if the cosmic ray events which accumulate on the CCD over long integrations have to be identified and corrected for.

A Programme to Simulate Observations with EFOSC2 and EMMI

S. D'ODORICO, J.-L. PRIEUR, G. RUPPRECHT, ESO

Introduction

Every astronomer appreciates the importance of preparing accurately an observing run to optimize the use of the time assigned at the telescope. The preparation implies, among other things, the selection of the observing mode which is best suited to the needs of the scientific programme and the computation of the signal-to-noise ratios (SNRs) one can achieve in a given observing time on the selected targets.

Instrumental models have been developed especially for space instruments to simulate the data obtainable at the telescope and to help in the detailed planning of the sequence of the observations. The possibility of a full simulation is relatively less common with

ground-based telescopes. At ESO, would-be observers have still to rely on the information of the Operating Manuals and do their own computations. This has the disadvantage that the parameters of the instruments are not available in digital form, that a change in the instrument configuration or in the detectors cannot be taken promptly into account and that the results of the computation of the final SNRs come in as many flavours as the number of astronomers.

As a first step in building a set of models which will describe the behaviour of the mostly used instruments at ESO one of us (J.L.P.) has developed in MIDAS a simulation programme for observations with EFOSC2 and EMMI,

two new ESO instruments which are about to come into general use at the NTT. EFOSC2 (eventually to be assigned to the 2.2-m telescope) has the same operating modes as EFOSC, the well-known focal reducer at the Cassegrain focus of the 3.6-m. EMMI is a more complex device which offers the possibility to select in real time among several observing modes. A description is attached to the ESO Call for Applications for Observing Time for period 45. The properties of EFOSC2 (such as the transmission of the optics, of the grisms, etc.) have been fully measured in the laboratory and can be used in the simulation. In the case of EMMI the data set is not complete and a realistic simulation will be working from March 1990